IPN Progress Report 42-234 • August 15, 2023

Extracting the UT1-UTC Earth Orientation Parameter from VLBA Multi-baseline Observing Sessions in the VGOS Database

Nikki A. Zivkov,* Durgadas S. Bagri,* Konstantin V. Belov,* Christopher S. Jacobs,* Gabor E. Lanyi,* Charles J. Naudet,* and Alexander S. Tolstov*

ABSTRACT. — This report discusses the creation of an automated pipeline to estimate the Earth Orientation Parameter (EOP) UT1-UTC from Very-Long Base Array (VLBA) multi-baseline observing sessions within the Very-Long Baseline Interferometry Global Observing System (VGOS) database. UT1-UTC accounts for accumulated errors in the length of day and is necessary to build reference frames for deep space navigation, guidance, and communications. In this report, we describe the modernization of the Jet Propulsion Laboratory (JPL) very-long baseline interferometry (VLBI) processing pipeline to use the open-source VGOS database [1]. The new pipeline built around the MODEST processor yields UT1-UTC estimates from VLBA multi-baseline observations comparable to published results from NASA's Crustal Dynamics Data Information System (CDDIS) and single-baseline Time and Earth Motion Precision Observations (TEMPO). Detrended residuals from VLBA multi-baseline UT1-UTC have a root mean square (RMS) of 33.7 microseconds, while residuals from single-baseline TEMPO UT1-UTC have an RMS of 40 microseconds. The improvement of this pipeline, including refined tropospheric estimates, updated references frames, and precise station locations, is ongoing.

I. Overview: Deep Space Navigation and Error in the Length of Day

A. Introduction

The new pipeline created for extracting UT1-UTC from multi-baseline Very-Long Base Array (VLBA) observing sessions in the open-source Very-Long Baseline Interferometry Global Observing System (VGOS) database has the potential to increase the significance of existing scientific applications of UT1-UTC, particularly through increased precision over long periods of observation. UT1-UTC, in combination with reference frames and other Earth Orientation Parameters (EOPs), is effective in deriving properties of the Galaxy and various geodetic parameters [2][3]. Additionally, UT1-UTC is an essential component of the International Celestial Reference Frame (ICRF) and the International Terrestrial

* Deep Space Tracking Systems Section.

The research described in this publication was carried out by the Jet Propulsion Laboratory, California Institute of Technology, under a contract with the National Aeronautics and Space Administration. © 2023 California Institute of Technology. U.S. Government sponsorship acknowledged.

Reference Frame (ITRF) [4][5]. Almost every navigational and telecommunications system, including all active spacecraft, rely on UT1-UTC for their temporal calibration [6].

Very-long baseline interferometry (VLBI) observations can be single-baseline, using only two telescopes with a distance between them, or multi-baseline, using more than two telescopes separated by distances relative to each other; the separation between telescopes is referred to as a baseline [7]. NASA's Deep Space Network (DSN) is a space telecommunications and flight operations system consisting of three radio telescope sites placed strategically across the Earth to guide, navigate, and communicate with spacecraft [8]. Additional VLBI networks of radio telescopes, which can be accessed through the VGOS database, aid the DSN by supplementing spacecraft navigation and providing precise observations to extract navigational parameters [9]. One such network is the Very-Long Baseline Array (VLBA), a VLBI network consisting of ten 25-meter-diameter radio telescopes spanning across the United States and U.S. Virgin Islands [8]. When all ten VLBA telescopes are used, the network provides 45 independent baselines. The DSN is a separate group of telescopes and baselines than the VLBA and other VGOS networks.

B. Universal Time: Error in the Length of Day

EOPs "describe the irregularity of the Earth's rotation [10]." There are three primary EOPs: rotation axis orientation in two Cartesian directions and UT1-UTC. For unique characterization of irregular axis motion, it is necessary to include an additional two celestial nutation axis offset parameters. Universal Time 1 (UT1) is a sidereal time derived from an angle measurement of the Sun's position with respect to the z-coordinate axis proportional to the angle of rotation of the Earth, corrected for polar wandering (Figure 1a). Over time, this angle changes slightly; the Earth does not rotate with perfect uniformity [11]. International Atomic Time (TAI) is a rotationally independent time based on the constant rate of Cesium-133 decay [12]. Universal Time Coordinated (UTC) differs from constant TAI due to the irregular rotation rate of the Earth, as seen in Figure 1b. Leap seconds are added or subtracted back onto UTC, as needed, in order to maintain a consistent timescale proportional to the accepted solar day and rotational adjustments of

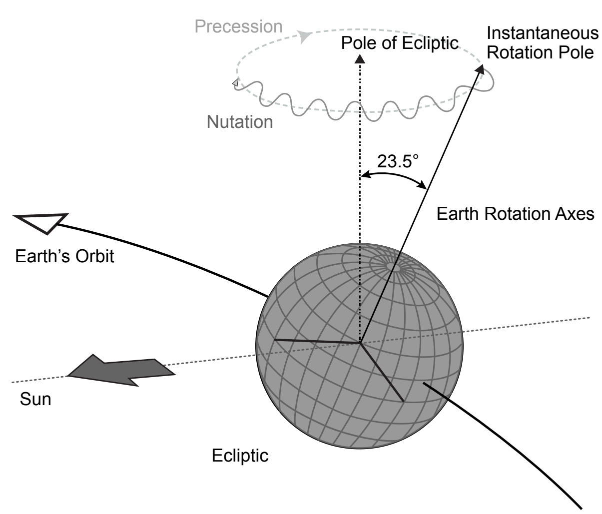

Figure 1a. Orientation of the Earth in the ecliptic plane. Image courtesy of Krzysztof Sośnica [14].

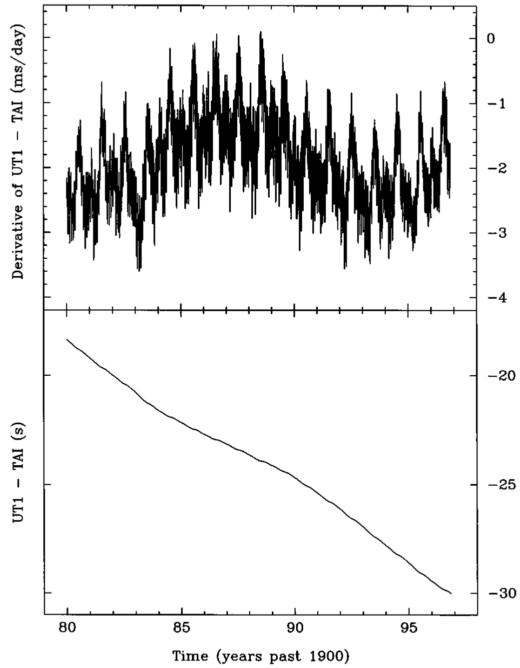

Figure 1b. Top plot shows the increase in the length of day with time in years, and the bottom plot shows the discrepancy in time measured by atomic clocks and the Earth's rotation [2].

the Earth [13]. The difference between UT1 and UTC is referred to as the accumulated error in the length of day, or UT1-UTC.

II. Extracting Multi-baseline UT1-UTC in MODEST

A. Previous Methods of Extracting UT1-UTC

Currently, JPL's Deep Space Tracking Systems Group calculates UT1-UTC primarily by processing single-baseline observing sessions through the MODEST processor. This software analysis pipeline intakes VLBI data then applies physical modelling and parameter estimation to extract EOPs [15]. Historically, DSN's UT1-UTC has been extracted on the single-baseline from the DSN's Goldstone and Madrid stations [9]. Using exclusively DSN assets ensures reliability, efficiency, and accuracy, all of which are necessary for precise deep space navigation. Additionally, single-baseline observations can yield less experimental and processing error for certain EOPs; it is simpler to correct poor residuals when a user is processing data between two telescopes as opposed to ten.

However, DSN single-baseline observations, which are independent from the VLBA and other VGOS multi-baseline networks, also produce EOPs that lack geometric coverage and temporal resolution. EOPs are extracted from single-baseline DSN observations approximately twice a month, whereas EOPs are extracted from multi-baseline VLBA observations daily. Additionally, processing UT1-UTC from single-baseline observations requires parameter estimation constraints, reducing the accuracy of the residuals. Because UT1-UTC is on the order of a fraction of a second, any small improvement to the data set, such as an additional baseline or extended observing period, may improve the precision of the result. It is hypothesized that multiple continental baselines, as utilized in extracting UT1-UTC from the VLBA, have the potential to perform with improved accuracy compared to the single intercontinental baseline between DSN stations used for TEMPO UT1-UTC. Multi-baseline processing from the VGOS database will not serve to replace single-baseline processing from the DSN because the DSN consistently provides effective EOPs; instead, it may serve as another method for yielding precise and accurate EOPs from observational data.

B. Obtaining Multi-baseline VLBA Data

VLBI, in combination with satellite data, is the only space geodetic technique currently capable of calculating all EOPs with enough accuracy for DSN operational support. The Global Navigation Satellite System (GNSS) yields nutation and polar motion EOPs with greater accuracy than VLBI techniques, while VLBI's geodetic technique yields UT1-UTC [16] [10]. Each VLBA station is located at a different point on the Earth's surface and will receive a radio signal from the source, a radio-loud quasar, at slightly different times [17] [18]. The signal delay, τ, is derived through signal correlation and will indicate the time delay between signals reaching each end of the interferometer. Combining time delay with additional information will yield EOPs, including UT1-UTC [2].

To develop the software pipeline to extract EOPs from multi-baseline observing sessions in the MODEST processor, VLBA multi-baseline sessions were downloaded from the VGOS database hosted by the Internal VLBI Service for Geodesy and Astronomy (IVS) [19]. The VGOS database is based on an open-source network Common Data Form (NetCDF) available through most operating systems [1]. The output yields UT1-UTC processed from 60 multi-baseline, 24-hour VLBA sessions spanning from January 2014 to December of 2018, approximately a 5-year period. The specific observing dates were chosen with the following restrictions: exclusively sessions within the NASA operations center, sessions that are fully released, and sessions that contain all necessary ancillary data files MODEST requires for processing.

C. Script Changes in MODEST to Estimate UT1-UTC from Multi-baseline Data

1. Constraints

MODEST utilizes constraints that restrict a parameter to limit its change relative to a base point. All key constraints are located in Appendix I. The first constraint is on nutation, which describes the periodic variation in the axis of the Earth's rotation [20]. Tropospheric parameters are also constrained to account for the troposphere's effect on incoming electromagnetic radiation. Both the wet and dry troposphere are refractive and alter an incoming, or outgoing, signal's direction and speed [21] [22]. To further control the troposphere, tropospheric gradients and the rate of change for north and east tropospheric gradients are tightly constrained to a priori values [15].

2. Fixed Parameters

Key fixed parameters are located in Appendix III. Constraining parameters as opposed to fixing them can be ineffective if said parameters fluctuate too frequently within the period of observation. In this solution, the X, Y, and Z Cartesian coordinates of each VLBA station were fixed to a priori values from ITRF 2008 [23] [5]. Additionally, a priori values were set for clock offset, epoch, and rate with no deviation.

Each quasar source is classified as defining or non-defining. Defining sources are internationally recognized by the International Astronomical Union (IAU) and have been observed multiple times with a uniform span across the sky; non-defining sources are not well established in MODEST's source catalog [24]. This lack of precision introduces extraneous noise to the output and will increase the uncertainty on UT1-UTC. To avoid this error, defining sources are fixed while non-defining sources are solved for within MODEST. Tidal parameters were also fixed in this solution. As tides shift, the Earth's crust experiences a linear pulling and pushing. This process will inevitably change the positions of each station [25]. To prevent tidal interference, specifically the effect on tectonic plate motion, the parameter solving for UT1 tidal amplitudes is ignored as well; this process will omit slow Universal Time and Polar Motion (UTPM) corrections, which are adjustments to UT1 over a five-day or shorter period [15].

3. Macros

MODEST incorporates several input directive groups, referred to as macros, which facilitate easy implementation for frequent use. Key macros are located in Appendix II. To solve for UT1-UTC, the UTPM pre-defined macro is included. This macro initiates solving for UT1-UTC, the X-coordinate of polar motion, and the Y-coordinate of polar motion with corresponding errors and correlation coefficients for each.

4. Cable Calibration and Ambiguity Correction

Signals from quasar sources are correlated between VLBA stations through cables, all of which must be calibrated for accuracy. These calibrations are typically performed in post-processing prior to inputting files into the VGOS database. To correlate signals between stations, and subsequently derive time delay, the complex components of an incoming signal are correlated. If each station is observing over a constant period of time, over a continuous range of bands, there are enough samples across the band to correlate signals effectively. However, if there are breaks in an observation, or large gaps in the channel, it is possible to miscount the integer cycles of a particular phase. This results in an ambiguity, also classified as an uncertainty in the group delay [26]. The following results were produced with cable calibration and ambiguity corrections included.

III. Analyzing: Extracting Multi-baseline UT1-UTC in MODEST

A. Introduction

The final analysis excludes outliers above and below 250 microseconds of the linear trend fit for UT1-UTC output extracted from each VLBA multi-baseline session from 2014–2018. The remaining experimental data includes 52 out of 60 VLBA multi-baseline sessions. To determine whether UT1-UTC output is reasonable, UT1-UTC is compared with published values from NASA's Crustal Dynamics Data Information System (CDDIS). CDDIS amalgamates observational data from various sources, both ground-based and satellite, to build a database of the most precise and accurate EOPs [27]. For the purpose of this report, values and errors for EOPs listed in NASA's CDDIS will be considered published truth. Prior to comparison, each CDDIS UT1-UTC value and error was interpolated through a cubic spline to match the modified Julian date (MJD) of MODEST's output. Residuals are calculated by subtracting CDDIS UT1-UTC values from MODEST UT1-UTC values. Output from VLBA multi-baseline sessions processed through MODEST are additionally compared to single-baseline sessions processed through Time and Earth Motion Precision Observations (TEMPO) in MODEST [28].

B. Experimental Analysis

Figure 2 shows detrended residuals for UT1-UTC processed from VLBA multi-baseline sessions. Detrended residuals are estimated by removing a linear-fit model from each residual. The root mean square (RMS) of the detrended residuals from the 52 VLBA sessions is 33.7 microseconds, while the RMS of the UT1-UTC error is 8.3 microseconds. The RMS of the corresponding single-baseline TEMPO processed through MODEST with 675 data points is approximately 50 microseconds without bias and rate removed, and 40 microseconds with bias and rate removed [29]. Additionally, experimental multi-baseline UT1-UTC matches CDDIS UT1-UTC to a minimum precision of milliseconds, with many matches on the order of nanoseconds. Reference Table 1 for specific comparisons. For all sessions, the percentage difference between MODEST UT1-UTC and interpolated CDDIS UT1-UTC averages to 0.48 microseconds.

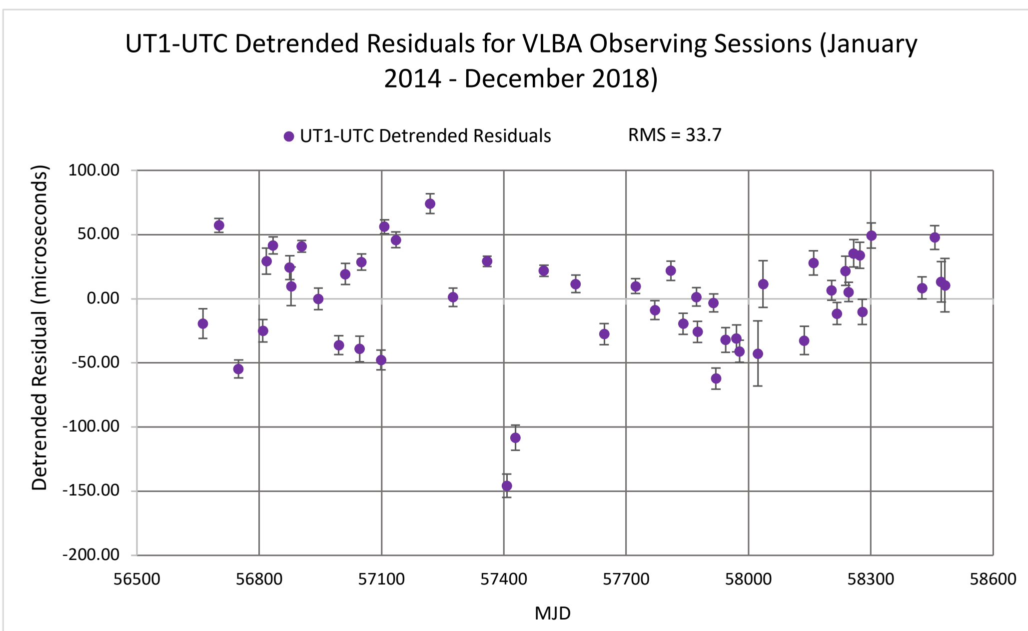

Figure 2. Detrended residuals from 5 years of VLBA sessions. Detrended residuals are calculated by computing the difference between MODEST multi-baseline processed UT1-UTC and interpolated UT1-UTC from CDDIS, then removing a linear-fit model.

C. Primary Conclusions

The primary goal of this experiment was to establish a pipeline for UT1-UTC to be extracted from VLBA multi-baseline observing sessions within the VGOS database and processed through MODEST. Overall, detrended residuals from UT1-UTC processed from single-baseline TEMPO yield higher RMS compared to detrended residuals from UT1-UTC processed from multi-baseline VLBA sessions. Additionally, the RMS from multi-baseline VLBA UT1-UTC is within an error margin of the RMS from single-baseline TEMPO UT1-UTC. The analysis software pipeline to extract multi-baseline UT1-UTC from VLBA data is new in comparison to the refined pipeline for extracting single-baseline TEMPO. Multi-baseline outputs from the new software analysis pipeline are viable in comparison to TEMPO with the potential to improve after more developments are made. Additional comparisons to CDDIS published data confirm the software analysis pipeline for extracting UT1-UTC from multi-baseline VLBA sessions is effective relative to previous methods.

IV. Future Work and Applications

A. Future Work and Sources of Error

1. Fixed Parameters

Fixed parameters within the input cards introduce a potential source of error. In a completely accurate solution, all parameters need to be accounted for in their entirety. It will be necessary to test how changing all fixed parameters to a priori constraints may improve UT1-UTC output.

2. Nutation

EOPs are determined by five angles, two for nutation, one for Universal Time, and two for polar motion. In processing UT1-UTC through MODEST, some nutation components were constrained to a priori values. However, there are relatively small, stochastically variable components of nutation; these deviations in nutation are not accounted for in the constrained a priori model. MODEST also does not account for the sinusoidal changes in free core nutation [20]. Other groups analyzing EOPs processed from VLBI observations predict that “weighted RMS errors of nutation residuals are minimally reduced 36%” when the free core nutation model and nutation correction components are estimated [30].

3. Interpolation Technique

To compare CDDIS UT1-UTC with MODEST UT1-UTC, CDDIS UT1-UTC were interpolated. This study utilized a cubic spline interpolation. This model was sufficient to produce a reasonable CDDIS UT1-UTC output; however, it does not make allowance for known harmonic terms contained within Universal Time, nutation, and tidal parameters. An improved model, such as a quadratic fit, will likely reduce the discrepancy between published and experimental UT1-UTC.

4. Global Solution

In this experiment, UT1-UTC is extracted through MODEST by processing each multi-baseline session individually; this can be defined as an individual solution. Conversely, a global solution is one in which sessions are combined to elongate the time period for which the data are collected. These sessions are processed together to produce EOPs. A global solution is a more effective method of extracting UT1-UTC because, as previously discussed, observing for longer periods generally produces higher quality datasets.

References

[1] J. Gipson, "IVS working group 4: VLBI data structures," *IVS 2010 General Meeting Proceedings*, pp. 187–191, 2012. https://ivscc.gsfc.nasa.gov/publications/gm2010/gipson3.pdf

[2] O. J. Sovers, J. L. Fanselow, and C. S. Jacobs, "Astrometry and geodesy with radio interferometry: experiments, models, results," *Reviews of Modern Physics*, vol. 70(4), pp. 1393–1454, 1998. https://doi.org/10.1103/revmodphys.70.1393

[3] M. J. Reid, "Structure and kinematics of the milky way," *Proceedings of the International Astronomical Union,* 13(S336), pp. 148–153, 2017. https://doi.org/10.1017/s1743921317009140

[4] "The international celestial reference frame," *International Earth Rotation and Reference System Service,* Federal Agency for Cartography and Geodesy, 2013. Accessed June 19, 2021. https://www.iers.org/IERS/EN/DataProducts/ICRF/ICRF/icrf.html

[5] "The international terrestrial reference frame," *International Earth Rotation and Reference System Service,* Federal Agency for Cartography and Geodesy, 2013. Accessed June 19, 2021. https://www.iers.org/IERS/EN/DataProducts/ITRF/itrf.html

[6] M. Telcide and P. Kwan, "Leap second and Earth orientation parameters," *Public Interface Control Working Group & Public Forum*. Lecture presented at the Space and Missile Symptoms Center Global Positioning Systems Directorate, 2019. Accessed December 30, 2022. https://www.gps.gov/technical/icwg/meetings/2019/05/presentation.pdf

[7] "Interferometry," European Southern Observatory. Accessed November 2, 2022. https://www.eso.org/public/teles- instr/technology/interferometry/

[8] P. J. Napier, J. A. Zensus, and P. J. Diamond, "The VLBA design," *Very Long Base Interferometry and the VLBA,* Astronomical Society of the Pacific Conference Series, vol. 82, p. 59, January 1995. https://articles.adsabs.harvard.edu/pdf/1995ASPC...82...59N

[9] V. I. Altunin, G. M. Resch, D. H. Rogstad, and P. R. Wolken, "VLBI in the deep space network: challenges and prospects," *IVS 2000 General Meeting Proceedings*, pp. 355–360, 2000. https://ivscc.gsfc.nasa.gov/publications/gm2000/altunin.pdf

[10] G. Petit and B. Luzum, "IERS conventions (2010)," IERS Conventions Centre, January 2010. https://www.iers.org/SharedDocs/Publikationen/EN/IERS/Publications/tn/TechnNote36/tn36.pdf?__blob=publicationFile&v=1

[11] S. Aoki, H. Kinoshita, B. Guinot, G. H. Kaplan, D. D. McCarthy, and P. K. Seidelmann, "The new definition of Universal Time," *Astronomy and Astrophysics,* vol. 105(2), pp. 359–361, January 1982. https://ui.adsabs.harvard.edu/abs/1982A%26A...105..359A

[12] K. Bikos and A. Buckle, "International atomic time," *International Atomic Time (TAI),* n.d. Accessed September 3, 2021. https://www.timeanddate.com/time/international-atomic-time.html

[13] P. Schlyter, "Timescales," *Time Scales: UT1, UTC, TAI, ET, TT, GPS time,* September 30, 2017. Accessed March 30, 2022. https://www.stjarnhimlen.se/comp/time.html

[14] K. J. Sosnica, "Determination of precise satellite orbits and geodetic parameters using satellite laser ranging," University of Bern, April 2014. http://www.bernese.unibe.ch/publist/2014/book/diss_ks_front.pdf

[15] O. J. Sovers, "MODEST user manual," JPL Internal Document, Jet Propulsion Laboratory, Pasadena, California, January 2009.

[16] R. Haas, E. Varenius, S. Matsumoto, and M. Schartner, "Observing UT1-UTC with VGOS," *Earth, Planets and Space,* vol. 73(1), March 25, 2021. https://doi.org/10.1186/s40623-021-01396-2

[17] W. J. Hurd, "Demonstration of intercontinental DSN clock synchronization by VLBI," *NASA Technical Reports Server,* NASA, January 1, 1973. https://static1.squarespace.com/static/55f05c0ce4b03bbf99b13c15/t/615ef103b485df67203a66b9/1633612036537/Demonstration+of+Intercontinental+DSN+Clock+Synchronization+by+VLBI.pdf

[18] M. Schartner, L. Kern, A. Nothnagel, J. Bohm, and B. Soja, "Optimal VLBI baseline geometry for UT1-UTC intensive observations," *Journal of Geodesy*, vol. 95(75), n.d. https://doi.org/https://doi.org/10.1007/s00190-021-01530-8

[19] W. Schluter and D. Behrend, "The International VLBI Service for geodesy and astrometry (IVS): current capabilities and future prospects." *Journal of Geodesy*, vol. 81, pp. 379–387, January 11, 2007. https://doi.org/https://doi.org/10.1007/s00190-006-0131-z

[20] "Free core nutation," *Special Bureau for the Core,* Global Geophysical Fluids Center, n.d. Accessed April 17, 2022. http://sbc.oma.be/freecornu.html

[21] "Tropospheric delay," *Tropospheric Delay,* European Space Agency, January 13, 2013. Accessed August 4, 2021. https://gssc.esa.int/navipedia/index.php/Tropospheric_Delay

[22] J. V. Sickle and J. A Dutton, "The Tropospheric Effect," *The Tropospheric Effect: GPS and GNSS for Geospatial Professionals,* Penn State College of Earth and Mineral Sciences. Accessed August 16, 2022. https://www.e-education.psu.edu/geog862/node/1719

[23] C. S. Jacobs, M. B. Heflin, G. E. Lanyi, O. J. Sovers, and J. A. Steppe, "Rotational alignment altered by source position correlations," *Sixth International VLBI Service for Geodesy and Astronomy*. Proceedings from the 2010 General Meeting, p. 305, December 2010. https://ivscc.gsfc.nasa.gov/publications/gm2010/jacobs2.pdf

[24] P. Charlot, C. S. Jacobs, D. Gordon, S. Lambert, A. de Witt, J. Böhm, A. L. Fey, R. Heinkelmann, E. Skurikhina, O. Titov, E. F. Arias, S. Bolotin, G. Bourda, C. Ma, Z. Malkin, A. Nothnagel, D. Mayer, D. S. MacMillan, T. Nilsson, and R. Gaume, "The third realization of the international celestial reference frame by very long baseline interferometry," *Astronomy & Astrophysics*, p. 644, 2020. https://doi.org/10.1051/0004-6361/202038368

[25] "Tide analysis," Virginia Institute of Marine Science, n.d. Accessed August 3, 2021. https://www.vims.edu/research/units/labgroups/tc_tutorial/tide_analysis.php

[26] P. W. Gorham, "Designing optimal bandwidth synthesis arrays for VLBI," *TMO Progress Report*, vol. 42-133, Jet Propulsion Laboratory, Pasadena, California, May 15, 1998. https://ipnpr.jpl.nasa.gov/progress_report/42-133/133D.pdf

[27] J. M. Bosworth, "The NASA Crustal Dynamics Project's use of satellite laser ranging and lunar laser ranging," *NASA Crustal Dynamics Project,* 2014. https://cddis.nasa.gov/lw19/docs/2014/Presentations/3132_Bosworth_presentation.pdf

[28] R. S. Gross, D. H. Boggs, J. O. Dickey, S. H. Oliveau, T. F. Runge, and J. A. Steppe, "Tempo: determining, combining, and predicting earth orientation parameters for spacecraft navigation," *Geodesy on the Move*, pp. 325–325, 1998. https://doi.org/10.1007/978-3-642-72245-5_48

[29] J. T. Ratcliffe, Personal Communication, March 8, 2023.

[30] P. Zhu, S. A. Triana, J. Rekier, A. Trinh, and V. Dehant, "Quantification of corrections for the main lunisolar nutation components and analysis of the free core nutation from VLBI-observed nutation residuals," *Journal of Geodesy,* vol. 95(5), 2021. https://doi.org/10.1007/s00190-021-01513-9

APPENDICES

I. Constraints within /dat6/zivkov/VLBA_5_marge_midnight/clean/18APR08XC.isl

Nutation constraint

```
APRIORI,NUTATION AMPLTD PSI C***,1.D+08
APRIORI,NUTATION AMPLTD EPS S***,1.D+08
APRIORI,NUTATION AMPLTD PSI S***,1.D+08
APRIORI,NUTATION AMPLTD EPS C***,1.D+08
```

II. Macros within /dat6/zivkov/VLBA_5_marge_midnight/clean/18APR08XC.isl

UTPM macro

```
C    UTPM
MACRO,utpm,
START,X POLE MOTION,,,
START,Y POLE MOTION,,,
START,UT1 MINUS UTC,,,
ENDMACRO,
```

III. Fixed parameters within /dat6/zivkov/VLBA_5_marge_midnight/18APR08XC.isl

Source parameters

```
C    ##### SOURCES_BEGIN #####
C     Fixed source positions
C    ##### SOURCES_END #####
C    ##### APRIORI_RA_DEC_BEGIN #####
IGNORE ,RIGHT ASCEN.************,
IGNORE ,DECLINATION ************,
C    ##### APRIORI_RA_DEC_END #####
C    ##### SOURCE_RATES_BEGIN #####
C   Source rates
C   Ignore sources with <20 obs., <5 year span
IGNORE ,DRASCEN/DT**************,
IGNORE ,DDECLIN/DT**************,
C    ##### SOURCE_RATES_END #####
```

Clock parameters

```
C     Clocks
C    ##### CLOCKS_BEGIN #####
APRIORI,C EPOCH ****************,1.D-0,,
APRIORI,C RATE  ****************,1.D-0,,
APRIORI,F OFFSET****************,1.D-0,,
IGNORE ,DCRAT/DTBR-VLBA     NOAM,
IGNORE ,DCRAT/DTDSS 43      AUST,
IGNORE ,DCRAT/DTFD-VLBA     NOAM,
IGNORE ,DCRAT/DTHARTRAO     AFRC,
IGNORE ,DCRAT/DTHOBART26    AUST,
IGNORE ,DCRAT/DTKP-VLBA     NOAM,
IGNORE ,DCRAT/DTLA-VLBA     NOAM,
IGNORE ,DCRAT/DTMK-VLBA     PCFC,
IGNORE ,DCRAT/DTNL-VLBA     NOAM,
IGNORE ,DCRAT/DTOV-VLBA     NOAM,
IGNORE ,DCRAT/DTPI-VLBA     NOAM,
IGNORE ,DCRAT/DTSC-VLBA     CARB,
IGNORE ,F DRIFT ****************,
IGNORE ,C EPOTMP****************,
C    ##### CLOCKS_END #####
```

Tidal parameters

```
C    ##### TIDAL_BEGIN
IGNORE ,UT1 TIDAL AMPLITUDE C***,
IGNORE ,UT1 TIDAL AMPLITUDE S***,
IGNORE ,PMX TIDAL AMPLITUDE C***,
IGNORE ,PMX TIDAL AMPLITUDE S***,
IGNORE ,PMY TIDAL AMPLITUDE C***,
IGNORE ,PMY TIDAL AMPLITUDE S***,
C   APRIORI,UT1 TIDAL AMPLITUDE ****,1.D0,,
C   APRIORI,PMX TIDAL AMPLITUDE ****,1.D0,,
C   APRIORI,PMY TIDAL AMPLITUDE ****,1.D0,,
IGNORE ,UT1 TIDAL AMPLITUDE CS1 ,
IGNORE ,UT1 TIDAL AMPLITUDE SS1 ,
IGNORE ,UT1 TIDAL AMPLITUDE CM1 ,
IGNORE ,UT1 TIDAL AMPLITUDE SM1 ,
IGNORE ,PMX TIDAL AMPLITUDE CS1 ,
IGNORE ,PMX TIDAL AMPLITUDE SS1 ,
IGNORE ,PMX TIDAL AMPLITUDE CM1 ,
IGNORE ,PMX TIDAL AMPLITUDE SM1 ,
IGNORE ,PMY TIDAL AMPLITUDE CS1 ,
IGNORE ,PMY TIDAL AMPLITUDE SS1 ,
IGNORE ,PMY TIDAL AMPLITUDE CM1 ,
IGNORE ,PMY TIDAL AMPLITUDE SM1 ,
C    ##### TIDAL_END #####
```

Table 1. 52 multi-baseline 2014-2018 VLBA sessions processed in MODEST for UT1-UTC and error, compared to interpolated CDDIS UT1-UTC and error.

CDDIS standard errors correspond to the rounded MJD from MODEST's session output. Experimental residuals are calculated by subtracting interpolated CDDIS UT1-UTC values from UT1-UTC processed in MODEST, then detrended residuals are computed by subtracting experimental residuals from the linear trend fitted residuals. All values are in microseconds.

Observing Sessions	MODEST UT1-UTC	MODEST UT1-UTC Error	Interpolated CDDIS UT1-UTC	CDDIS UT1-UTC Standard Error	Detrended Residual	Detrended Residual Error
14JAN04XC	-102255.58	9.09	-102141.01	7.10	-19.37	11.53
14FEB12XA	-140883.03	2.70	-140696.26	4.80	57.33	5.51
14APR01XA	-206934.81	6.16	-206865.51	3.30	-54.68	6.99
14MAY31XC	-282808.83	6.84	-282716.51	5.60	-24.82	8.84
14JUN09XC	-288143.12	8.35	-287997.52	6.00	29.44	10.28
14JUN25XA	-300922.74	4.37	-300766.82	5.00	41.63	6.64
14AUG05XC	-316377.93	8.68	-316243.94	3.40	24.35	9.32
14AUG09XC	-316953.96	10.80	-316834.80	10.50	9.91	15.06
14SEP03XA	-328979.00	3.33	-328831.74	2.90	40.96	4.42
14OCT14XA	-368240.51	3.94	-368138.83	7.50	0.04	8.47
14DEC03XA	-427603.43	5.94	-427543.60	4.30	-36.11	7.33
14DEC20XC	-446143.39	6.12	-446029.93	5.50	19.39	8.23
15JAN23XC	-484641.98	6.88	-484590.88	7.20	-39.01	9.96
15JAN28XA	-490353.76	5.21	-490235.56	3.40	28.65	6.22
15MAR17XC	-550187.22	6.73	-550150.85	3.90	-47.76	7.78
15MAR25XA	-567161.47	2.53	-567022.05	4.80	56.25	5.43
15APR22XA	-607590.50	3.36	-607464.61	5.10	45.92	6.11
15JUL15XA	309474.93	4.89	309619.57	6.10	74.25	7.82
15SEP09XA	259866.68	5.65	259932.00	4.50	1.30	7.22
15DEC02XA	128770.01	3.18	128853.74	2.60	29.29	4.11
16JAN19XA	44430.19	8.49	44333.34	2.90	-145.81	8.98
16FEB09XA	12846.18	7.31	12784.40	6.40	-108.35	9.72
16APR19XA	-119087.58	2.71	-119027.09	3.30	21.89	4.27
16JUL06XA	-216522.35	5.59	-216480.99	3.90	11.66	6.82
16SEP14XA	-258608.23	4.91	-258613.92	6.60	-27.41	8.23
16NOV30XA	-370017.13	3.56	-369994.33	4.60	9.85	5.82
17JAN16XC	569094.13	6.09	569092.76	4.20	-8.93	7.40
17FEB24XC	522155.69	5.59	522180.72	5.10	21.90	7.56
17MAR27XC	478404.01	6.03	478384.19	5.70	-19.48	8.30
17APR28XC	424282.52	6.03	424279.87	3.90	1.39	7.18
17MAY01XC	420099.25	7.05	420069.15	4.40	-25.73	8.31
17JUN10XC	371204.52	6.18	371192.49	3.40	-3.16	7.05
17JUN15XC	368623.16	7.05	368551.52	4.20	-62.12	8.20
17JUL09XC	357411.16	7.07	357366.90	6.60	-32.08	9.67
17AUG05XC	346083.98	7.04	346037.85	7.60	-30.88	10.36
17AUG12XC	342784.22	7.17	342727.24	4.60	-40.87	8.52

Observing Sessions	MODEST UT1-UTC	MODEST UT1-UTC Error	Interpolated CDDIS UT1-UTC	CDDIS UT1-UTC Standard Error	Detrended Residual	Detrended Residual Error
17SEP26XC	317637.81	24.07	317573.95	8.40	-42.66	25.49
17OCT09XC	306477.95	18.00	306466.78	2.10	11.54	18.12
18JAN18XC	207695.68	7.22	207628.99	8.30	-32.46	11.00
18FEB09XC	183623.30	8.05	183614.63	4.90	28.10	9.42
18MAR26XC	140663.87	6.65	140628.81	3.90	6.77	7.71
18APR08XC	127028.41	6.37	126973.63	5.70	-11.46	8.54
18APR29XC	102579.77	9.12	102555.76	6.90	21.75	11.44
18MAY07XC	96499.00	6.08	96457.70	4.30	5.32	7.45
18MAY19XC	85980.97	6.57	85968.36	8.50	35.42	10.74
18JUN03XC	76148.42	7.74	76132.60	6.60	33.88	10.17
18JUN09XC	71878.05	7.06	71817.47	6.70	-10.14	9.73
18JUL01XC	71347.91	8.84	71344.36	4.30	49.40	9.83
18NOV03XC	16340.12	6.18	16281.43	5.90	8.45	8.54
18DEC04XC	-16745.10	7.20	-16767.91	6.00	47.85	9.37
18DEC20XC	-27364.62	15.45	-27423.71	3.20	13.39	15.78
18DEC29XC	-33959.35	19.83	-34022.25	6.80	10.64	20.96